

AD-A035 361

DAVID W TAYLOR NAVAL SHIP RESEARCH AND DEVELOPMENT CE--ETC F/G 13/10
BLADE SPINDLE MOMENT ON A FIVE-BLADED CONTROLLABLE-PITCH PROPEL--ETC(U)
JAN 72 S B DENNY, J J NELKA

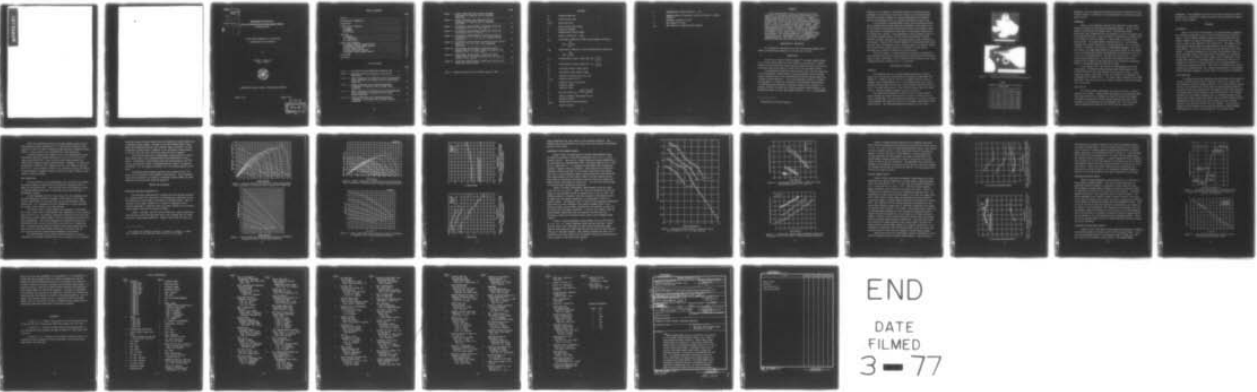
UNCLASSIFIED

SPD-3729

NL

| OF |

AD
A035361



END

DATE
FILMED
3 - 77



MICROCOPY RESOLUTION TEST CHART
NATIONAL BUREAU OF STANDARDS-1963-A

ADA035361

ASSIGN for	
White Section	<input checked="" type="checkbox"/>
Buff Section	<input type="checkbox"/>
UNCLASSIFIED	<input type="checkbox"/>
DISTRIBUTION/AVAILABILITY CODES	
SPECIAL INSTRUCTIONS	
A	

DEPARTMENT OF THE NAVY
 NAVAL SHIP RESEARCH AND DEVELOPMENT CENTER
 BETHESDA, MD. 20034

BLADE SPINDLE MOMENT ON A FIVE-BLADED
 CONTROLLABLE-PITCH PROPELLER

by

Stephen B. Denny and
 John J. Nelka



APPROVED FOR PUBLIC RELEASE: DISTRIBUTION UNLIMITED

January 1972

Report 3729

DDC
 RECEIVED
 FEB 9 1977
 D

TABLE OF CONTENTS

	Page
ABSTRACT	1
ADMINISTRATIVE INFORMATION	1
INTRODUCTION	1
DESCRIPTION OF APPARATUS	2
PROPELLER	2
DYNAMOMETRY	4
TEST FACILITY	4
PROCEDURE	5
CALIBRATION	5
TEST CONDITIONS	5
DATA ACQUISITION	8
RESULTS AND DISCUSSION	9
OPEN-WATER PROPELLER CHARACTERISTICS	9
HYDRODYNAMIC SPINDLE-MOMENT RESULTS	13
REYNOLDS NUMBER EFFECTS	16
PROPELLER CAVITATION EFFECTS	18
CENTRIFUGAL SPINDLE-MOMENT RESULTS	18
CONCLUSIONS	20
REFERENCES	22

LIST OF FIGURES

	Page
Figure 1 - Five-Bladed Controllable-Pitch Propeller 4402	3
Figure 2 - Operating Conditions Simulated in the Tunnel Experiments	7
Figure 3 - Thrust Coefficient and Efficiency Curves Showing Open- Water Performance of Propeller 4402 at Steady Ahead Conditions	10
Figure 4 - Torque Coefficient Curves Showing Open-Water Performance of Propeller 4402 at Steady Ahead Conditions	10
Figure 5 - Thrust Coefficient and Efficiency Curves Showing Open- Water Performance of Propeller 4402 at Steady Backing Conditions	11
Figure 6 - Torque Coefficient Curves Showing Open-Water Performance of Propeller 4402 at Steady Backing Conditions	11

	Page
Figure 7 - Thrust Coefficient Data Showing Open-Water Performance of Propeller 4402 at Crashback Conditions	12
Figure 8 - Torque Coefficient Data Showing Open-Water Performance of Propeller 4402 at Crashback Conditions	12
Figure 9 - Hydrodynamic Spindle-Moment Coefficient Curves for P/D Ratios of 1.4, 1.2, 1.061, and 0.8	14
Figure 10 - Hydrodynamic Spindle-Moment Coefficient Curves for P/D Ratios of 0.6, 0.4, and 0.2	15
Figure 11 - Hydrodynamic Spindle-Moment Coefficient Curves for P/D Ratios of -0.3, -0.5, and -0.7 (Steady Backing Conditions)	15
Figure 12 - Hydrodynamic Spindle-Moment Coefficient Curves for P/D Ratios of 0.0, -0.4, and -1.061 (Crashback Conditions)	17
Figure 13 - Hydrodynamic Spindle-Moment Coefficient Curves Showing Effects of Reynolds Number Variation for P/D Ratios of 1.4, 1.2, 1.061, and 0.8	17
Figure 14 - Hydrodynamic Spindle-Moment Coefficient Curves Showing Effects of Blade Cavitation for P/D Ratio of 1.061, $J = 0.5$, and 0.8	19
Figure 15 - Centrifugal Spindle-Moment Coefficient Curves for the Blade Pitch Ratios Tested	19
Table 1 - Geometry Characteristics of Model Propeller 4402	3

NOTATION

A_E	Expanded blade area
A_O	Propeller disk area
A_E/A_O	Blade area ratio
c	Blade section chord length
D	Propeller diameter
f	Maximum blade section camber
J	Advance coefficient, $J = \frac{V}{nD}$
K_{MC}	Centrifugal component of blade spindle-moment coefficient, $K_{MC} = \frac{M_C}{\rho_B n^2 D^5}$
K_{MH}	Hydrodynamic component of blade spindle-moment coefficient, $K_{MH} = \frac{M_H}{\rho n^2 D^5}$
K_Q	Nondimensional torque coefficient, $K_Q = \frac{Q}{\rho n^2 D^5}$
K_T	Nondimensional thrust coefficient, $K_T = \frac{T}{\rho n^2 D^4}$
M_C	Centrifugal blade spindle moment
M_H	Hydrodynamic blade spindle moment
n	Propeller revolutions per unit time
$P_{0.7R}$	Propeller pitch at 0.7R
P	Propeller blade section pitch
Q	Propeller torque
R	Propeller radius
R_n	Reynolds number, $R_n = \frac{c \sqrt{V^2 + (2\pi nr)^2}}{\nu}$
r	Radial coordinate from propeller axis
T	Propeller thrust
t_{max}	Maximum blade section thickness
V	Speed of advance

x	Nondimensional radial position $x = r/R$
γ	Angular position of propeller blade with respect to design location
ν	Kinematic viscosity of water
ρ	Mass density of water
ρ_B	Mass density of propeller-blade material

ABSTRACT

Blade spindle-moment values are presented for the operation of a five-bladed controllable-pitch propeller over a range of blade pitches and advance conditions. Spindle moment (blade turning effort) was measured on a single blade of NSRDC Model Propeller 4402 in an experimental program conducted in the 24-in. variable-pressure water tunnel. Experimental results are presented as mean spindle-moment values taken at steady-state operating conditions. No transient or time-dependent data were taken. The operating conditions investigated include (1) positive pitch--steady ahead, (2) negative pitch--steady backing, and (3) negative pitch--ahead advance. The spindle moment due to hydrodynamic loading and that due to centrifugal forces were separated and nondimensionalized. The effects of Reynolds number and propeller blade cavitation are discussed briefly.

ADMINISTRATIVE INFORMATION

This program was sponsored by the Naval Ship Systems Command (NAV-SHIPS) and funded under Subproject SF 35 432 008, Task 3741.

INTRODUCTION

The success of previous NSRDC attempts^{1,2} to measure spindle moment (i.e., blade turning effort) has been limited by the inability to experimentally isolate the spindle moment-measuring mechanism from the effects of extraneous blade forces (thrust, torque force, and centrifugal force).

A calculation procedure³ has been available since 1961 for predicting (1) the hydrodynamic spindle moment at design propeller pitch and design advance condition and (2) the centrifugal-force-induced spindle moment for a range of pitch conditions. It has been impossible, however, to extend this procedure to include the calculation of hydrodynamic spindle moment at off-design pitch and advance conditions because of the inability to properly describe the radial and chordwise propeller blade loading in the mathematical model at other than design conditions. This is understandable

¹References are listed on page 22.

inasmuch as (1) attempts to theoretically predict off-design propeller performance itself have met with little success and (2) spindle-moment prediction logically requires an accurate representation of chordwise pressure distribution as well as a precise description of radial load.

A safe estimate of spindle-moment limits can be obtained by manipulating experimentally obtained open-water performance data (steady state and transient), resolving the blade forces involved, and choosing a point of application on the propeller blade which is sufficiently removed from the spindle axis location. The disadvantage of this procedure, however, is the strength (weight) aspect; the full-scale blade spindles, turning mechanism linkages, and hydraulic actuating equipment would inevitably be overdesigned. Because of the current emphasis on increased delivered horsepower for naval and merchant vessels, auxiliary power and propeller weights are already critical quantities and an overdesign in blade-turning mechanism must certainly be avoided if at all possible.

For these reasons, it became necessary to develop instrumentation and procedures which could provide adequate determinations of blade spindle moment in model experiments. Such a system has been fabricated, and initial experimentation has indicated that it is successful.

DESCRIPTION OF APPARATUS

PROPELLER

The propeller used in all spindle-moment measurements reported herein was a five-bladed, controllable-pitch propeller, NSRDC Model 4402 (Figure 1). Propeller 4402 is 9.224 in. in diameter and has a hub-to-diameter ratio of approximately 0.29. Its aluminum blades have a blade thickness fraction equal to 0.059 and a total expanded blade area ratio of 0.829. The blade pitch ratio is 1.061 at the 70 percent propeller radius section. Detailed propeller geometry is given in Table 1.

The blades were constructed so that the axis of blade rotation passes through each radial blade section at a point 40 percent from the section leading edge. This construction method leads to a slight curvature of the midchord line from root to tip and a consequent induced skew of the blade sections. The resulting geometric peculiarities are of little

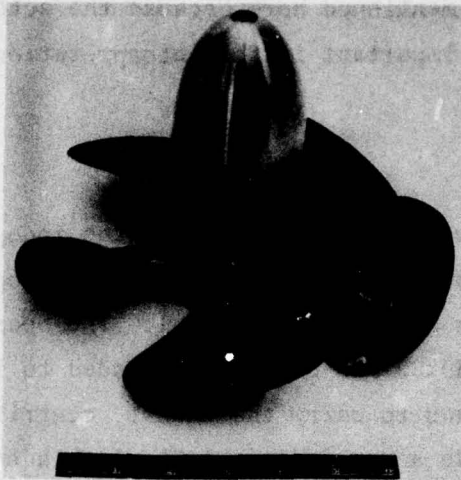


Figure 1a - Overall View

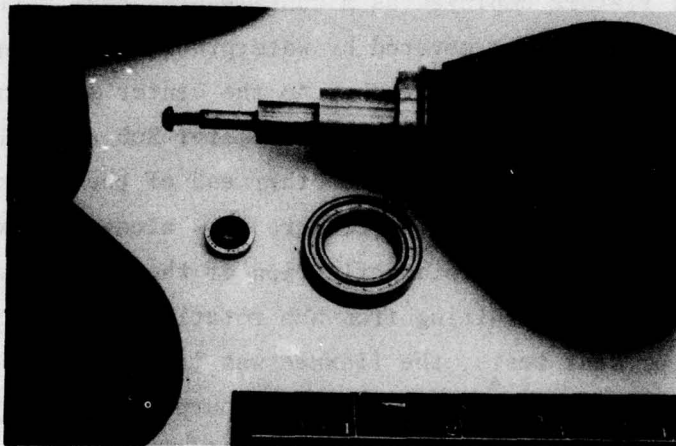


Figure 1b - Blade Spindle Mechanism

Figure 1 - Five-Bladed Controllable-Pitch Propeller 4402

TABLE 1
Geometry Characteristics of Propeller
Model 4402

x	P/D	c/D	t_{\max}/D	f/D
0.30	1.0083	0.1853	0.0436	0.0046
0.40	1.0444	0.2482	0.0327	0.0075
0.50	1.0667	0.3111	0.0250	0.0087
0.60	1.0722	0.3740	0.0186	0.0090
0.70	1.0611	0.4369	0.0130	0.0084
0.80	1.0250	0.4760	0.0089	0.0067
0.90	0.9639	0.4587	0.0061	0.0038
0.95	0.9222	0.4228	0.0051	0.0020

importance; they are mentioned here because the actual location of the axis of blade rotation is important in the interpretation of experimental spindle-moment results.

DYNAMOMETRY

Figure 1b shows Propeller 4402 with the independent blade spindle mechanism designed for the current experimental program. The hub, blade spindle, and bearings are stainless steel. The bearings (Barden Corporation Types A539X80 and SF2) are intended to isolate the spindle from the dynamometer hub and to carry the thrust, centrifugal, and torque forces on the propeller blade and spindle. A single blade is attached to the blade spindle. The spindle-moment measuring element is a strain-gaged tempered-steel flexure employed as a cantilevered beam. (It is not shown in Figure 1b because it is covered by waterproofing compound.) One end of the flexure is a clamp which attaches to the center section of the spindle; it can be adjusted from outside the dynamometer hub and allows blade pitch to be set at any desired value. The other end of the flexure rests in a close-tolerance ground slot. The flexure lies along the axis of the propeller hub in order to avoid deflection of the flexure and centrifugal forces on the flexure resulting from hub rotation.

In the present tests, the flexure was instrumented with 120-ohm strain gages. Excitation voltage and gage output were transmitted via slipring assemblies with leads through a hollow propeller shaft. Power supply and signal conditioning for the strain gages was accomplished with an ENDEVCO (Card 5) Model 4471.1. The output signal, amplified with a DANA Model 2850, was read directly from a digital voltmeter (Non-Linear Systems, Inc. Series 2900).

TEST FACILITY

All spindle-moment measurements were made in the 24-in. variable-pressure water tunnel. Propeller 4402 was mounted on the downstream shaft and blade pitches were set manually by using the construction template (70 percent section) and a vernier-scribed angle-setting device which attached to the upstream end of the dynamometer hub. The water tunnel setup incorporated the open-jet test section and the 150-hp tunnel

dynamometer. This dynamometer has thrust and torque limitations of 3000 lb and 300 ft-lb, respectively--quantities which were well beyond the demands of the current program.

PROCEDURE

CALIBRATION

Prior to the series of measurements, the spindle-moment dynamometry was statically calibrated in air at its installed position in the water tunnel. Positive moments (moments tending to increase blade pitch) and negative moments were applied incrementally to the spindle over a range twice as large as that expected in the actual tests. The response of the strain gages remained linear with applied moment, and the response was instantaneous. No hysteresis characteristics were observed in the output signal. It remained unchanged over the entire spindle-moment range as pure centrifugal, thrust, and torque forces were applied to the spindle. On the basis of the results of the stringent static calibrations, it was assumed that there was no extraneous force interaction and that the dynamometry was reliable for measuring mean values of spindle moment at steady-state operating conditions. When static calibrations were repeated following all experimentation, the response characteristics of the spindle-moment dynamometer appeared to be the same as in the earlier calibrations.

TEST CONDITIONS

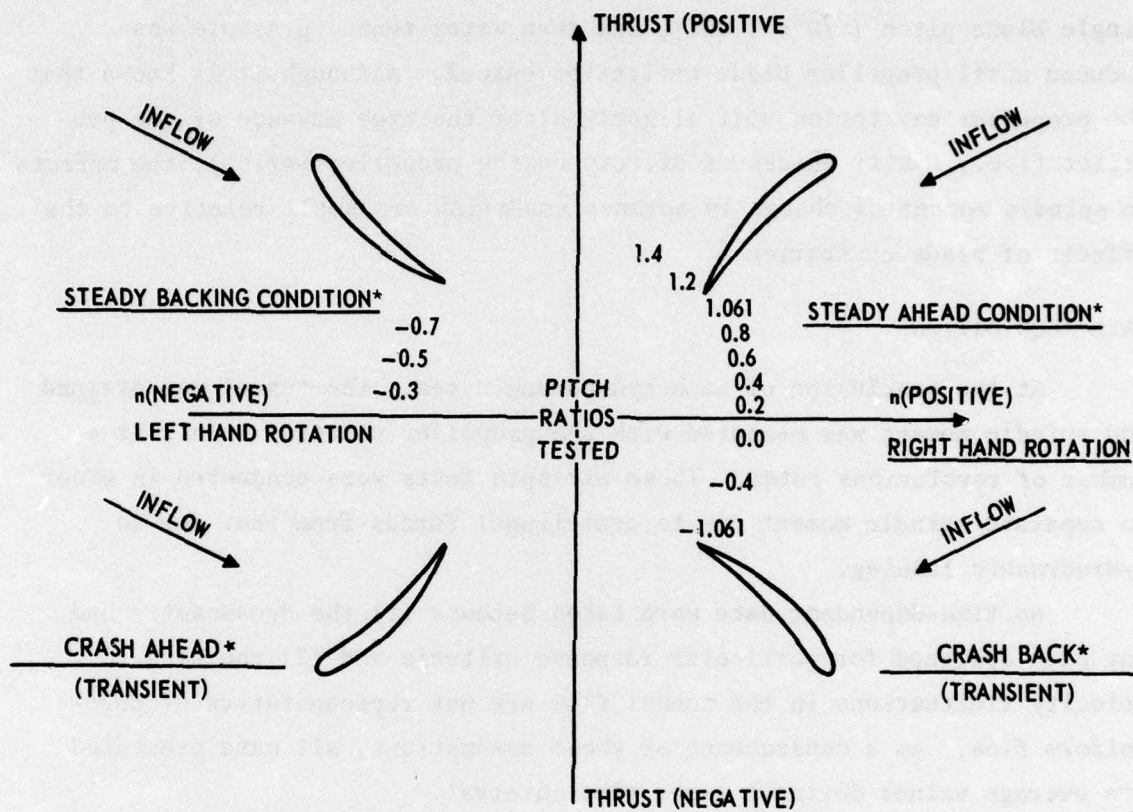
All propeller operating conditions were established in the tunnel by setting a thrust-identity with the open-water (basin test) results for a given propeller pitch and advance condition. For a given propeller angular velocity (in revolutions per second--rps) and desired advance condition, the water velocity was adjusted until the propeller thrust value (dictated by the open-water thrust coefficient curve) was achieved. This standard procedure for water-tunnel propeller tests is necessary because the propeller action itself distorts the tunnel flow and neither venturi pressure measurement nor pitot tube survey can be relied on to give accurate measure of the mean flow velocity into the propeller. The accuracy of propeller thrust readings and the resulting accuracy of spindle-moment measurements with such a test procedure will be discussed later.

Figure 2 is a schematic of the propeller operating conditions simulated in these experiments. The propeller pitch ratios (P/D values) are listed in the operating quadrants in which they were actually tested. The schematic deviates somewhat from what would ordinarily be expected in a "four-quadrant" explanation of inflow relative to a propeller. Since flow in the tunnel was limited to one direction, it was necessary to establish steady backing conditions by rotating the blades 180 deg and reversing the shaft rotation so that a positive thrust was produced just as in the case of positive-pitch, right-hand rotation. The crashback pitch condition shown in Figure 2 is self-explanatory; however, only limited results were obtained for crashback since the thrust of the propeller against the flow caused basic instabilities in the tunnel flow. In many cases it was impossible to achieve a particular crashback condition; the data presented herein are values which appeared to be repeatable and were judged steady enough to be reliable. A particular crashback condition can usually be achieved by reducing propeller rpm for a given advance condition and consequently reducing the magnitude of the generated thrust. However the extent to which rpm can be reduced is limited because of Reynolds number restrictions. A lowering of the effective Reynolds number appears to influence spindle-moment data considerably more than propeller thrust and torque coefficient data at the same conditions. A more detailed explanation of Reynolds number dependency will be given later.

As mentioned earlier, propeller blade pitch was set manually with the aid of construction templates. The differential angle from design pitch was determined with the following equation:

$$\gamma = \tan^{-1} \frac{[P/D] \text{ set}}{0.7\pi} - \tan^{-1} \frac{[P/D] \text{ design}}{0.7\pi}$$

with all pitch ratios defined at the 70 percent propeller radius. Calculations showed that for the spindle-moment values measured, the actual bending of the flexure in the dynamometer produced less than ± 0.1 deg of pitch change of the measuring blade assembly. This accuracy is as good as can realistically be expected when blade pitch is set by hand, as was done in these experiments.



*SIMULATED FULL SCALE CONDITIONS

Figure 2 - Operating Conditions Simulated in the Tunnel Experiments

Many test conditions were run at the same propeller pitch and the same propeller advance coefficient J ($J = V/nD$) but for different combinations of V and n in order to explore the possibilities of Reynolds number effects. These results will be elaborated on in the discussion.

Cavitation studies were limited to only a few representative cases. A particular propeller advance condition ($J = 0.8$ or 0.5) was set for a single blade pitch ($P/D = 1.061$), and then water-tunnel pressure was reduced until propeller blade cavitation ensued. Although it is known that the propeller cavitation will slightly alter the true advance of the propeller (i.e., cavity thickness effects on the propeller inflow), the effects on spindle moment of change in advance condition are small relative to the effects of blade cavitation

DATA ACQUISITION

At the conclusion of each hydrodynamic test, the tunnel was drained and spindle moment was measured with the propeller rotating in air at a number of revolutions rates. These air-spin tests were conducted in order to separate spindle moment due to centrifugal forces from that due to hydrodynamic loading.

No time-dependent data were taken because (1) the dynamometry had not been designed for particular response criteria and (2) the slight velocity fluctuations in the tunnel flow are not representative of pure uniform flow. As a consequence of these assumptions, all data presented are average values during a 1-sec time interval.

The actual values of spindle moment were measured in inch-pounds, and in most steady cases the measurements were repeatable at 1-sec intervals within ± 0.02 in.-lb. The greatest inaccuracies observed in the tests were those which occurred during attempts to set a given propeller thrust on the tunnel dynamometer. The 150-hp dynamometer has inherent friction and a deviation of ± 0.05 lb from a given thrust value would not be unexpected. Such a variation between actual and desired thrust would produce true advance variations and spindle-moment differences far greater than the errors arising from the spindle-moment dynamometer inaccuracies.

The spindle-moment values which were measured were, of course, a combination of centrifugal spindle moment due to asymmetry of the propeller

blade mass about the blade spindle axis and hydrodynamic spindle-moment due to propeller blade loading. Although the air-spin spindle-moment values which were subtracted from the total measured signals contained a certain aerodynamic loading effect in addition to the centrifugal spindle-moment, it will be shown that these effects are small and can be ignored.

The separated quantities of hydrodynamic spindle moment and centrifugal spindle moment were nondimensionalized for presentation in this report. Hydrodynamic spindle-moment quantities were divided by $[\rho n^2 D^5]$ -- just as the propeller torque is nondimensionalized--where n is propeller revolutions, D is the propeller diameter, and ρ is the mass density of the fluid.

Centrifugal spindle-moment quantities were divided by $[\rho_b n^2 D^5]$ where ρ_b is the density of the propeller blade material. Such a procedure allows easier estimates to be made of centrifugal spindle moment for other propellers constructed from different materials.

RESULTS AND DISCUSSION

OPEN-WATER PROPELLER CHARACTERISTICS

The open-water characteristics of Model 4402 that had been obtained in a separate study* were utilized in establishing test conditions for the variable-pressure water-tunnel investigation of spindle moment. They are included in this report (Figures 3-6) to enable a comparison of the relative magnitudes of propeller thrust and torque loading to the resulting spindle-moment values for the propeller blades.

Figures 3 through 6 show the thrust coefficient, torque coefficient, and efficiency curves from open-water basin tests of Model 4402 in steady ahead and steady backing conditions. Figures 7 and 8 show the thrust and

*The authors are indebted to Messrs. R. Hecker, F. Puryear, A. Campo, and K. Remmers for the open-water data utilized in this report.

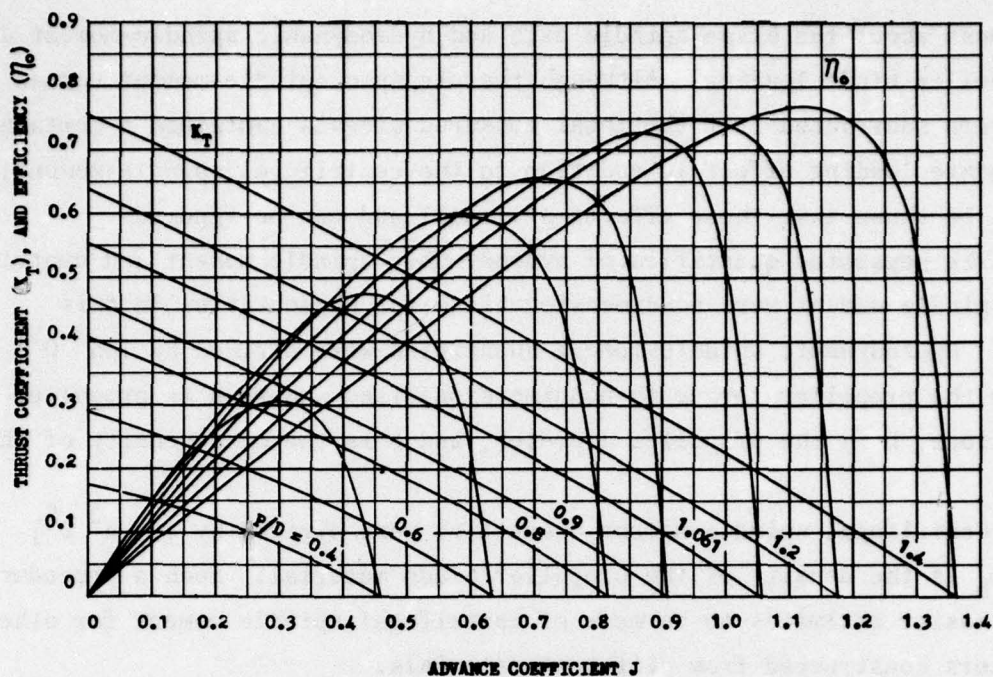


Figure 3 - Thrust Coefficient and Efficiency Curves Showing Open-Water Performance of Propeller 4402 at Steady Ahead Conditions

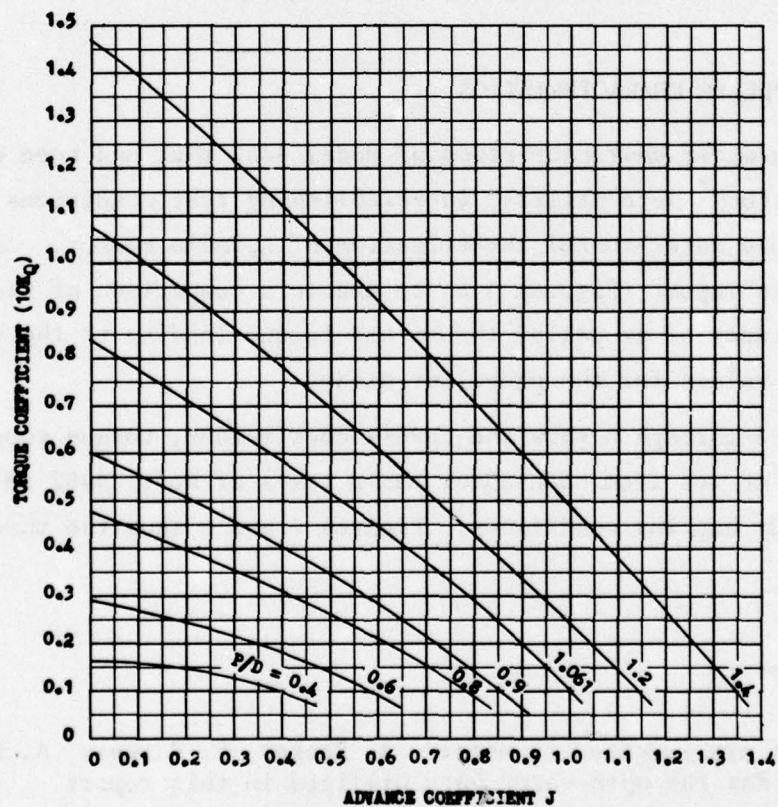


Figure 4 - Torque Coefficient Curves Showing Open-Water Performance of Propeller 4402 at Steady Ahead Conditions

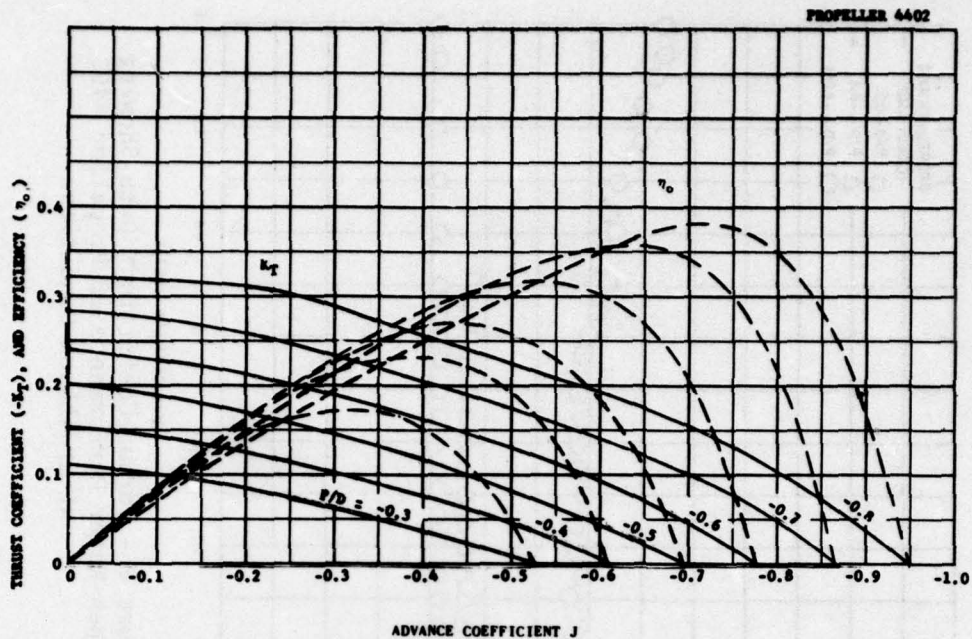


Figure 5 - Thrust Coefficient and Efficiency Curves Showing Open-Water Performance of Propeller 4402 at Steady Backing Conditions

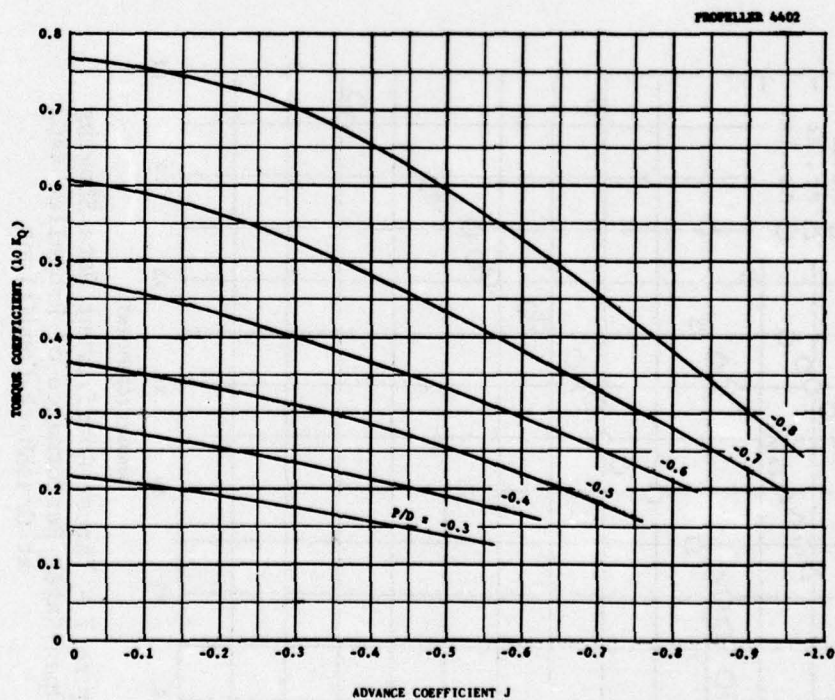


Figure 6 - Torque Coefficient Curves Showing Open Water Performance of Propeller 4402 at Steady Backing Conditions

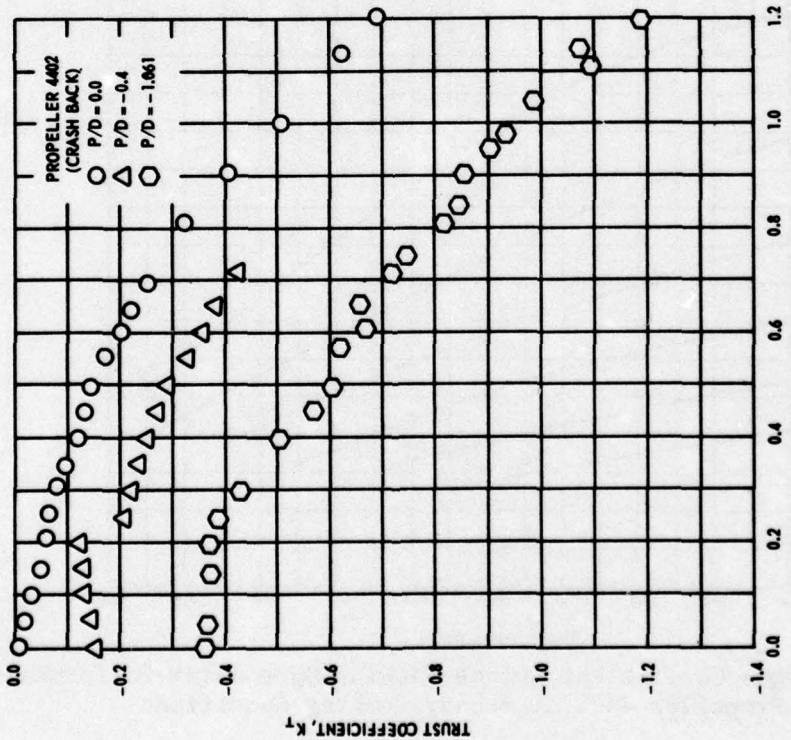


Figure 7 - Thrust Coefficient Data Showing Open-Water Performance of Propeller 4402 at Crashback Conditions

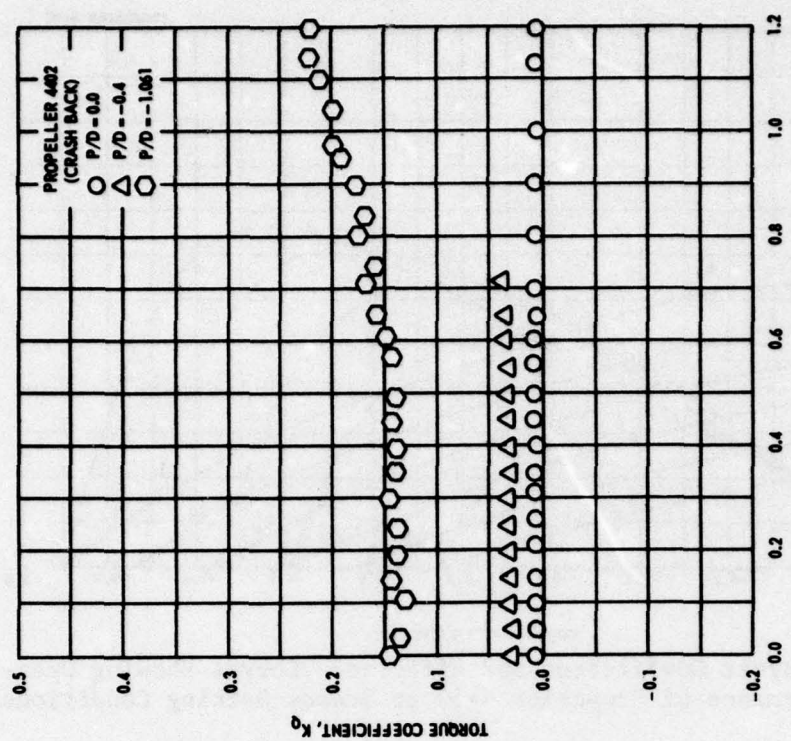


Figure 8 - Torque Coefficient Data Showing Open-Water Performance of Propeller 4402 at Crashback Conditions

torque coefficient test spot results in the crashback condition. The crashback data are presented as test spots only since there was considerable scatter in the results.

HYDRODYNAMIC SPINDLE-MOMENT RESULTS

Figure 9 shows the experimentally obtained spindle-moment values for propeller operation at four pitch conditions: $P/D = 1.4$, 1.2 , 1.061 (design), and 0.8 . Data are for a range of positive advance coefficients J and are expressed in nondimensional form. The values shown for $P/D = 1.061$ in the J range from $1.0 - 1.8$ represent spindle-moment data at propeller "windmill" (negative thrust) conditions. Since there were no open-water performance results with which to set tunnel conditions in this region, some error in establishing the advance condition may have resulted and the true spindle-moment curve may differ slightly from the reported results. Water speed was held fixed and propeller rpm was reduced to simulate the higher advance coefficients for these cases. All other data were obtained at known open-water performance conditions.

Figure 10 presents hydrodynamic spindle-moment curves for pitch ratios of 0.6 , 0.4 , and 0.2 . Again the curves are presented only for the ranges in which propeller thrust was greater than or equal to zero. Two different propeller revolution rates were explored in obtaining the data to demonstrate the apparent dependency of spindle-moment results on Reynolds number. The propeller rates of 20 and 25 rps represent sufficiently high values to ensure breakdown of the laminar boundary layer on the propeller blades, and the thrust coefficients were identical at these two rps values for each advance condition. It can be seen, however, that the spindle-moment coefficients were not identical and that they were definitely a function of resultant inflow velocity and consequent blade loading.

Figure 11 shows hydrodynamic spindle-moment data for pitch ratios of -0.3 , -0.5 , -0.7 during simulated steady backing conditions. Recall that for these tests, each blade had been rotated 180 deg from normal negative pitch positions (right-hand rotation) and that the shaft had been reversed to left-hand rotation. This procedure enabled the tests to be conducted in the water tunnel with the propeller delivering steady positive thrust relative to the tunnel flow velocity.

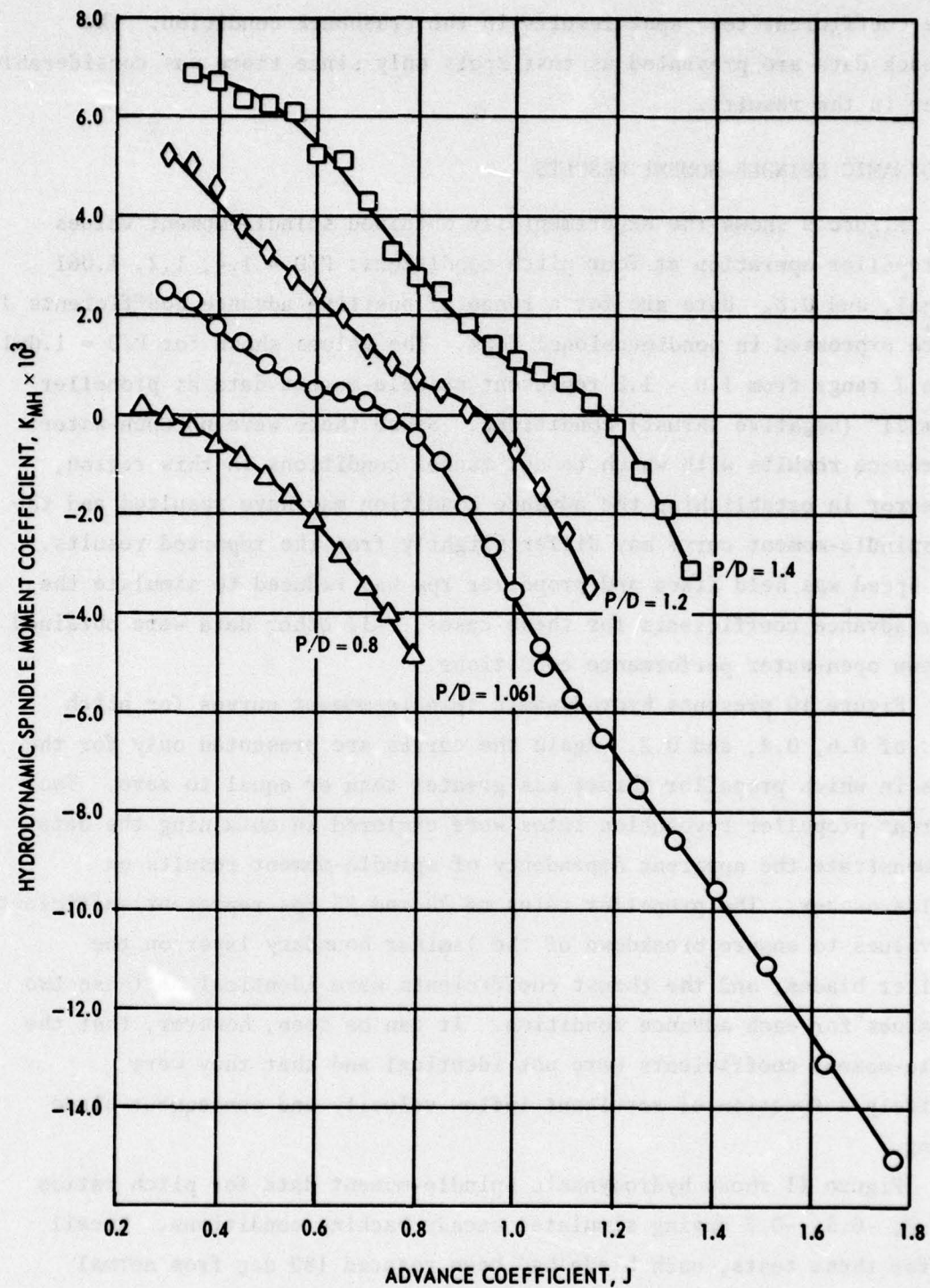


Figure 9 - Hydrodynamic Spindle-Moment Coefficient Curves for P/D Ratios of 1.4, 1.2, 1.061, and 0.8

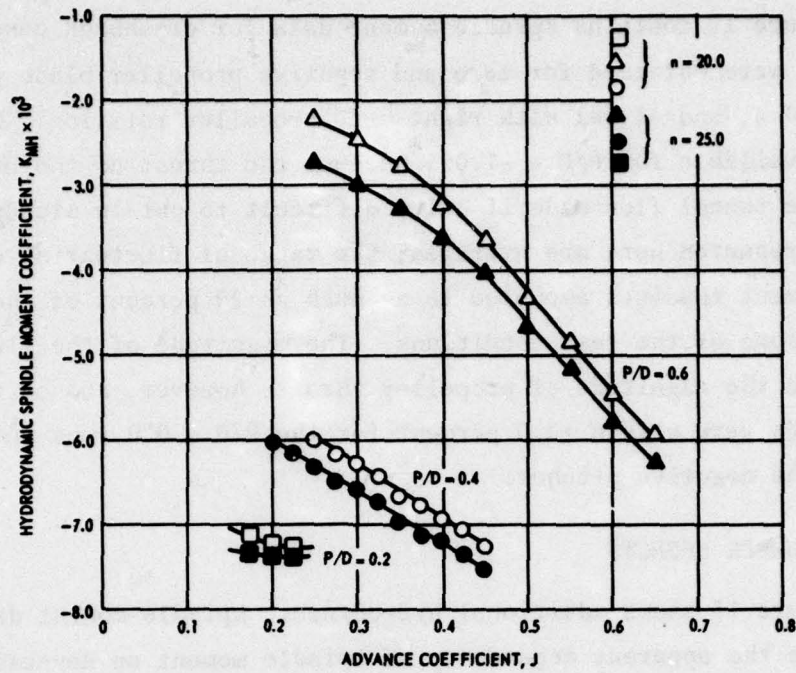


Figure 10 - Hydrodynamic Spindle-Moment Coefficient Curves for P/D Ratios of 0.6, 0.4, and 0.2

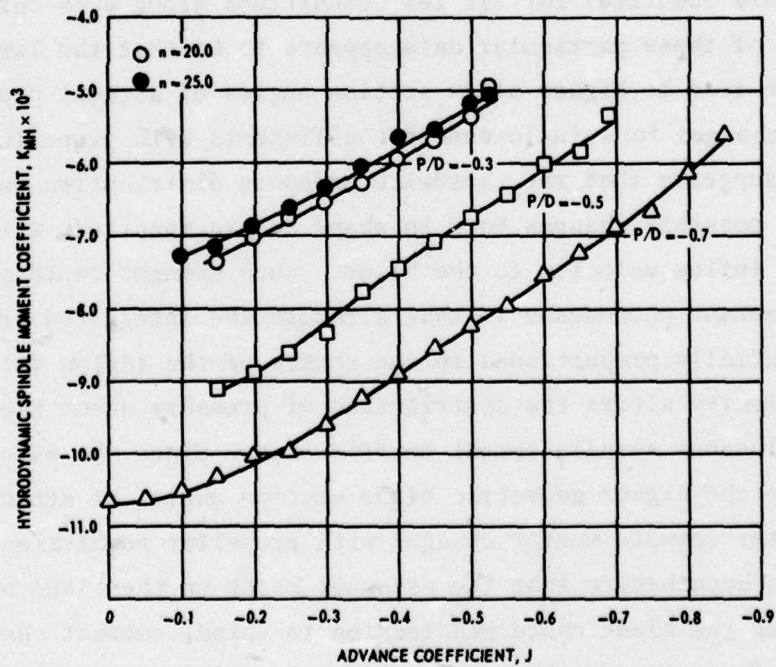


Figure 11 - Hydrodynamic Spindle-Moment Coefficient Curves for P/D Ratios of -0.3, -0.5, and -0.7 (Steady Backing Conditions)

Figure 12 contains spindle-moment data for crashback conditions. These data were obtained for zero and negative propeller blade pitch ratios of 0.0, -0.4, and -1.061 with right-hand propeller rotation. Only limited data are available for $P/D = -1.061$ because the thrust of the propeller against the tunnel flow made it quite difficult to obtain steady data. The data presented here are averages; the range of fluctuation of the spindle-moment readings amounted to as much as 20 percent of the total signal at some of the test conditions. The magnitude of the fluctuation depended on the magnitude of propeller thrust, however, and on the average, the readings were within ± 2.0 percent for the $P/D = 0.0$ runs and ± 6.0 percent for the negative pitches.

REYNOLDS NUMBER EFFECTS

Figure 13 shows additional hydrodynamic spindle-moment data which demonstrate the apparent dependency of spindle moment on Reynolds number. Curves are given for $P/D = 1.4, 1.2,$ and 1.061 at an advance coefficient of $J = 0.8$ and for $P/D = 0.8$ at $J = 0.5$. The plots indicate spindle-moment coefficient versus propeller revolutions per second. Thrust coefficients were identical for all test conditions along each curve. The significance of these particular data appears to be that the larger pitch ratios (which lead to higher blade section angles of attack) produced the greater changes in spindle-moment coefficients with propeller rotation rate. This suggests that the chordwise pressure distribution on a propeller blade possibly changes both in shape and in magnitude with changes in resultant inflow velocity to the blade. Such changes could account for the spindle-moment phenomenon in that although the integrated pressure remains essentially proportional to the square of the inflow velocity, a change in velocity alters the distribution of pressure about the spindle axis and influences spindle-moment coefficients. Since the pitch ratios which produce the higher geometric blade section angles of attack also produce greater spindle moment changes with propeller revolutions, it is reasonable to hypothesize that the pressure peaks on the blade back were shifting along the blade chord and leading to spindle-moment changes.

Other factors were also considered as possible contributors to the effects designated above as Reynolds number effects. Typical factors

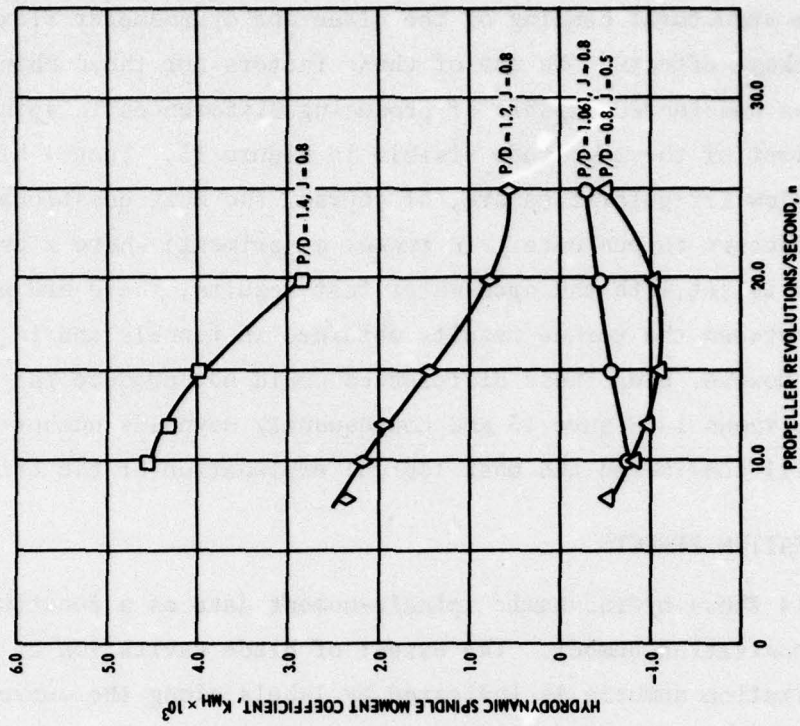


Figure 13 - Hydrodynamic Spindle-Moment Coefficient Curves Showing Effects of Reynolds Number Variation for P/D Ratios of 1.4, 1.2, 1.061, and 0.8

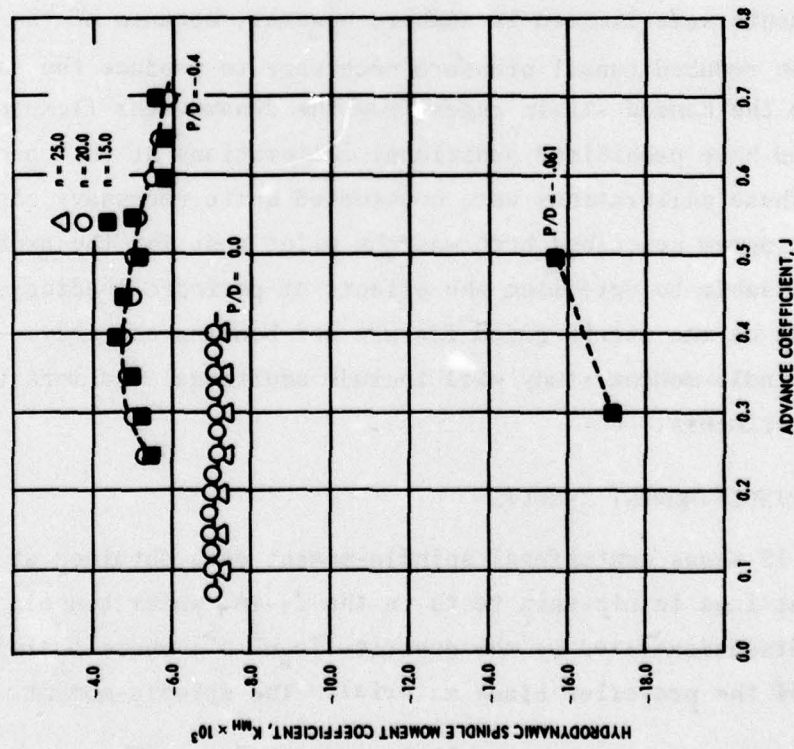


Figure 12 - Hydrodynamic Spindle-Moment Coefficient Curves for P/D Ratios of 0.0, -0.4, and -1.061 (Crashback Conditions)

considered were structural bending of the blade and dynamometer flexure and tunnel blockage effects. No one of these factors nor the combination of all three was considered capable of producing differences in spindle-moment coefficient of the magnitude visible in Figure 13. Tunnel blockage effects and inflow irregularities are, of course, the most questionable and difficult factors to evaluate. In tunnel experiments where a propeller thrust-identity is set with the open-water test results, there are usually discrepancies between the torque results obtained in tunnels and in basins (open water). However even these differences could not produce the characteristics shown in Figure 13 and consequently Reynolds number dependency is still considered the most logical explanation of the effect.

PROPELLER CAVITATION EFFECTS

Figure 14 shows hydrodynamic spindle-moment data as a function of blade section cavitation number. The extent of blade cavitation at particular cavitation numbers is indicated by labels along the curves. The variation in spindle-moment readings at particular cavitation numbers is depicted by the scatter in the plotted test spot symbols. Cavitation appears to have had a very significant effect on spindle moment. Cavitation experiments were limited in number, however, because of the possibility that the reduced tunnel pressure necessary to produce the cavitation would separate the bonded strain gages from the dynamometer flexure. Such a failure would have prohibited additional calibrations at the conclusion of testing. These calibrations were considered quite necessary since the experimental program described here was the pilot test for the dynamometer and it was advisable to determine the effects of periodic loading and the wet environment on the strain-gaged flexure and bearing assembly. Future work in the spindle-moment study will include additional and more thorough cavitation experiments.

CENTRIFUGAL SPINDLE-MOMENT RESULTS

Figure 15 shows centrifugal spindle-moment data obtained at different blade pitch settings in air-spin tests in the 24-in. water tunnel. These data were nondimensionalized by the quantity $[\rho_B n^2 D^5]$ where ρ_B is the mass density of the propeller blade material. The spindle-moment

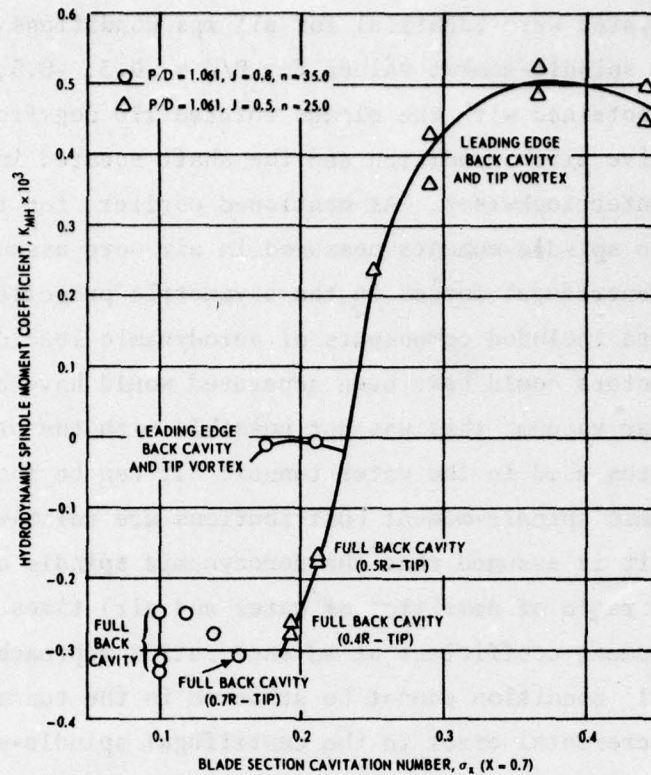


Figure 14 - Hydrodynamic Spindle-Moment Coefficient Curves Showing Effects of Blade Cavitation for P/D Ratio of 1.061, $J = 0.5$, and 0.8

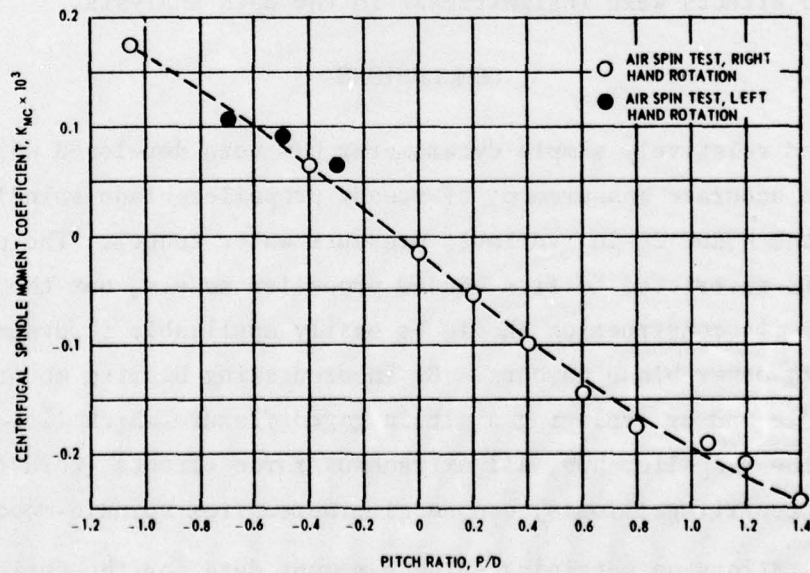


Figure 15 - Centrifugal Spindle-Moment Coefficient Curves for the Blade Pitch Ratios Tested

coefficients generated were identical for all rps conditions at a given pitch ratio. The spindle-moment values for $P/D = -0.3, -0.5, \text{ and } -0.7$ (Figure 15) were obtained with the blades rotated 180 deg from their appropriate negative pitch condition and the shaft rotated in the left-hand direction (or counterclockwise). As mentioned earlier, for the purpose of data analysis, the spindle-moments measured in air were assumed to be entirely due to centrifugal forces in the asymmetric propeller blade. Actually these data included components of aerodynamic loading. The only way that these factors could have been separated would have been to run the tests in a near vacuum; this was not possible with the pressure-regulating apparatus used in the water tunnel. It can be shown, however, that the aerodynamic spindle-moment contributions are relatively small. For instance, if it is assumed that the aerodynamic spindle moment is 0.001 (due to the ratio of densities of water and air) times the hydrodynamic spindle moment coefficient at advance ratios approaching zero (a true 'Bollard-Pull' condition cannot be achieved in the tunnel), then it is found that the incremental error in the centrifugal spindle-moment coefficient curve is less than 0.02. Noticeable scatter in the plotted centrifugal spindle-moment coefficient curve is approximately one-half of this value. As a consequence of these estimates, it was assumed that the aerodynamic effects were insignificant in the data analysis.

CONCLUSIONS

1. A new and relatively simple dynamometer has been developed which enables the accurate measurement of steady propeller-blade spindle moment in the NSRDC 24-in. variable-pressure water tunnel. The present apparatus is restricted to five-bladed propeller models, but the principles involved in its construction should be easily applicable to dynamometry systems with other blade numbers. By incorporating bearing mounts for the blade spindle and by employing a strain-gaged flexure which lies along the center of the propeller hub, all extraneous force effects (thrust, torque force, and centrifugal force) can be eliminated from spindle-moment data.
2. The limitations on obtaining spindle-moment data for the entire simulated operating range of a controllable-pitch propeller are imposed by the

water-tunnel facility itself and not by the spindle-moment dynamometer. The propeller action on the water-tunnel inflow generates unsteady inflow for certain crashback conditions, and makes low-speed inflow unachievable for low-advance, positive-pitch conditions. The number of achievable test conditions could be appreciably increased by adapting the dynamometry to the propeller testing apparatus used in the towing basin. However it is recommended that such an instrumentation development be postponed until the phenomena of Reynolds number and cavitation effects on spindle moment are fully examined.

3. Reynolds number based on resultant inflow to the blade section appears to produce a significant effect on propeller-blade spindle moment. Despite the fact that propeller thrust coefficients are constant at the same advance condition for a range of propeller revolutions and advance velocities, propeller-blade spindle-moment coefficients show considerable variation for different Reynolds numbers. It appears that a change in the magnitude of the inflow velocity to the propeller blade is accompanied by a shift in the pressure distribution on the propeller blade and that although the integrated pressure is proportional to the square of the inflow velocity, the distribution of pressure about the spindle axis is altered, thus yielding differences in spindle-moment with Reynolds number variation. Additional experimentation is recommended to determine appropriate test Reynolds number ranges for future model testing and for accurate prediction of full-scale spindle moment.

4. Propeller blade cavitation affects blade spindle moment considerably, but much more experimentation is necessary before any conclusions can be drawn concerning the relative effects of cavitation and blade loading on blade spindle moment.

5. Centrifugal spindle-moment data can be determined experimentally with the existing dynamometry. Spindle-moment data taken in air-spin tests can provide acceptable values of centrifugal spindle moment if the aerodynamic effects are ignored or estimated.

6. Funding has been obtained for additional experimental work to determine the effects of blade geometry on spindle moment. Blade area and blade

skew will be the first parameters to be considered. It is reasonable to assume that these parameters must be examined thoroughly and that the problem of Reynolds number effects must be solved before any attempt can be made to develop an analytic procedure for estimating spindle moment. As mentioned earlier, there are no known reliable procedures for predicting blade spindle moment at off-design conditions. The delay in developing such procedures has been due to an inability to describe the chordwise and radial pressure distributions on blades at off-design operation. Since it appears that Reynolds number also has a significant effect on spindle moment, then the state-of-the-art may be somewhat farther removed from an operational prediction method than was previously imagined.

REFERENCES

1. Miller, M.L., "Spindle Torque Tests of Four CRP Propeller Blade Designs for MSO 421," David Taylor Model Basin Report 1837 (Jul 1964).
2. Hansen, E.O., "Thrust and Blade Spindle Torque Measurements of Five Controllable-Pitch Propeller Designs for MSO-421," NSRDC Report 2325 (Apr 1967).
3. Boswell, R.J., "A Method of Calculating the Spindle Torque of a Controllable-Pitch Propeller at Design Conditions," David Taylor Model Basin Report 1529 (Aug 1961).

INITIAL DISTRIBUTION

<p>Copies 22</p>	<p>NAVSHIPS 1 SHIPS 2052 1 SHIPS 033 1 SHIPS 034 5 SHIPS 03413 1 SHIPS 037 1 SHIPS 2062 1 SHIPS 08 1 PMS 78 1 PMS 79 1 PMS 80 1 PMS 81 1 PMS 82 1 PMS 83 1 PMS 84 1 PMS 89 1 PMS 91 1 PMS 92 1 PMS 358</p>	<p>Copies 1</p>	<p>NAVSHIPYD BREM NAVSHIPYD PHILA NAVSHIPYD CHASN NAVSHIPYD LBEACH NUSC, Newport CDR, NELC CO & DIR USNAVCIVENGLAB DDC ADMIN, MARAD 1 Office of Ship Construction 1 Office of Res & Dev 1 Mr. E.S. Dillon 1 Mr. R. Kracht 1 Mr. R. Schubert 1 Mr. J. Nachtsheim 1 Mr. F. Dashnaw 1 Mr. Hammar</p>
<p>8</p>	<p>NAVSEC 1 SEC 6100 2 SEC 6110 1 SEC 6140 2 SEC 6144 2 SEC 6148</p>	<p>12 8</p>	<p>CO, USNROTC & NAVADMINUMIT USNAVPGSCOL, Monterey JSESPO SUPT, USNA SUPT, USMA CMDT, USCOGARD Attn: Ship Const Comm DIR, ORL, Penn State Attn: Dr. M. Sevik Chief of Res & Dev, Office of Chief of Staff, Dept of the Army, The Pentagon DIR, WHOI NASA, College Park Attn: Sci & Tech Info, Acquisitions Br Commanding General, Army Eng Res & Dev Lab, Fort Belvoir, Va., Attn: Tech Doc Cen Library of Congress Science & Technology Div Washington, D.C. 20540</p>
<p>1</p>	<p>NAVORDSYSCOM (ORD 05411)</p>	<p>1</p>	<p>SUPT, USNA</p>
<p>1</p>	<p>NAVSEC NORFOLK (Code 6660)</p>	<p>1</p>	<p>SUPT, USMA</p>
<p>2</p>	<p>CHONR 1 Fluid Dynamics (Code 438) 1 Sys & Res Gp (Code 492)</p>	<p>1</p>	<p>CMDT, USCOGARD Attn: Ship Const Comm</p>
<p>1</p>	<p>CDR, NURDC</p>	<p>1</p>	<p>DIR, ORL, Penn State Attn: Dr. M. Sevik</p>
<p>1</p>	<p>CDR, NWL</p>	<p>1</p>	<p>Chief of Res & Dev, Office of Chief of Staff, Dept of the Army, The Pentagon</p>
<p>1</p>	<p>CDR, USNOL</p>	<p>1</p>	<p>DIR, WHOI</p>
<p>1</p>	<p>DIR, USNRL</p>	<p>1</p>	<p>NASA, College Park Attn: Sci & Tech Info, Acquisitions Br</p>
<p>1</p>	<p>ONR, SAN FRAN</p>	<p>1</p>	<p>Commanding General, Army Eng Res & Dev Lab, Fort Belvoir, Va., Attn: Tech Doc Cen</p>
<p>1</p>	<p>CO, ONR, BSN</p>	<p>1</p>	<p>Library of Congress Science & Technology Div Washington, D.C. 20540</p>
<p>1</p>	<p>CO, ONR, Pasadena</p>	<p>1</p>	<p>Library of Congress Science & Technology Div Washington, D.C. 20540</p>
<p>1</p>	<p>CO, ONR, Chicago</p>	<p>1</p>	<p>Library of Congress Science & Technology Div Washington, D.C. 20540</p>
<p>1</p>	<p>CO, ONR, London</p>	<p>1</p>	<p>Library of Congress Science & Technology Div Washington, D.C. 20540</p>
<p>1</p>	<p>NAVSHIPYD PTSMH</p>	<p>1</p>	<p>Library of Congress Science & Technology Div Washington, D.C. 20540</p>
<p>1</p>	<p>NAVSHIPYD BSN</p>	<p>1</p>	<p>Library of Congress Science & Technology Div Washington, D.C. 20540</p>

Copies		Copies	
1	Univ of Bridgeport Bridgeport, Conn 06602 Attn: Prof. Earl Uram, Mech Engr. Dept.	1	Kansas State Univ Engr Experiment Station Seaton Hall Manhattan, Kansas 66502 Attn: Prof. D.A. Nesmith
2	Naval Architecture Department College of Engr Univ of Calif Berkeley, Calif 94720 1 Librarian 1 Prof. J.V. Wehausen	1	Lehigh Univ DE Bethlehem, Pa 18015 Attn: Fritz Laboratory Lib
3	Calif Inst of Tech. Pasadena, Calif 91109 1 Dr. A.J. Acosta 1 Dr. T.Y. Wu 1 Dr. M.S. Plesset	1	Long Island Univ Graduate Dept of Marine Sci 40 Merrick Avenue East Meadow, N.Y. 11554 Attn: Prof David Price
1	Univ of Connecticut Box U-37 Storrs, Conn. 06268 Attn: Prof. V. Scottorn Hydraulic Research Lab	1	MIT, Hydrodynamics Lab Cambridge, Mass 02139 Attn: Prof A.T. Ippen
1	Cornell Univ Graduate School of Aerospace Engineering Ithaca, New York 14850 Attn: Prof. W.R. Sears	6	MIT, Dept of Naval Arch & Marine Engr, Cambridge, Mass, 02139 1 Dr. A.H. Keil 1 Prof P. Mandel 1 Prof J.E. Kerwin 1 Prof P. Leehey 1 Prof M. Abkowitz 1 Dr. J.N. Newman
1	Harvard Univ 2 Divinity Avenue Cambridge, Mass. 02138 Attn: Prof. G. Birkhoff Dept of Mathematics	1	U.S. Merchant Marine Academy Kings Point, L.I., N.Y. 11204 Attn: Capt L.S. McCready Head, Dept of Engr
1	Univ of Ill College of Engr Urbana, Ill 61801 Attn: Dr. J.M. Robertson Theoretical & Applied Mechanics Dept	3	Univ of Michigan Dept of Naval Arch & Marine Engr Ann Arbor, Michigan 48104 1 Dr. T.F. Ogilvie 1 Dr. F.C. Michelson 1 Dr. H. Nowaki
1	The Univ of Iowa Iowa City, Iowa 52240 Attn: Dr. Hunter Rouse	5	St. Anthony Falls Hydraul Lab Univ of Minnesota Mississippi River at 3rd Ave., S.E. Minneapolis, Minn 55414 1 Director 1 Dr. C.S. Song 1 Mr. J.M. Killeen 1 Mr. F. Schiebe 1 Mr. J.M. Wetzel
2	The Univ of Iowa Iowa Inst of Hydraulic Res Iowa City, Iowa 52240 1 Dr. L. Landweber 1 Dr. J. Kennedy		

Copies

1 New York Univ
Univ Heights
Bronx, New York 10453
Attn: Prof W. Pierson, Jr.

2 New York Univ
Courant Inst of Math Sci
251 Mercier St
New York, New York 10012
1 Prof A.S. Peters
1 Prof J.J. Stoker

1 Colorado State Univ
Dept of Civil Engr
Fort Collins, Colorado 80521
Attn: Prof M. Albertson

2 Scripps Inst of Oceanography
Univ of Calif
La Jolla, Calif 92038
1 J. Pollock
1 M. Silverman

1 College of Engr
Utah State Univ
Logan, Utah 84321
Attn: Dr. Roland W. Jeppson

1 Stanford Univ
Stanford, Calif 94305
Attn: Prof H. Ashley
Dept of Aeronautics &
Astronautics

3 SIT, DL
711 Hudson Street
Hoboken, N.J. 07030
1 Dr. J.P. Breslin
1 Dr. S. Tsakonas
1 Library

1 Univ of Wash
Applied Physics Lab
1013 N.E. 40th St
Seattle, Wash 98105
Attn: Director

2 Webb Institute of Naval Arch
Crescent Beach Road
Glen Cove, L.I., N.Y. 11542
1 Prof E.V. Lewis
1 Prof L.W. Ward

Copies

1 Worcester Polytechnic Inst
Alden Research Labs
Worcester, Mass 01609
Attn: Director

1 Dept of Mathematics
St. John's Univ
Jamaica, New York 11432
Attn: Prof. Jerome Lurye

1 Univ of Notre Dame
Dept of Mech Eng

1 Rensselaer Polytechnic Inst,
Dept Mathe., Troy, N.Y.

2 JHU, Baltimore
1 Dept of Mechanics
1 Inst of Cooperative Res

2 State Univ of New York,
Maritime College
Bronx, N.Y.
1 Engr Dept
1 Inst of Math Sciences

1 Friede & Goldman, Inc
Suite 1414
225 Baronne Street,
New Orleans, La 70112
Attn: Mr. W.H. Michel

1 Pacific Far East Lines, Inc
141 Battery St
San Francisco, Calif 94111
Attn: Mr. G.J. Gmeich,
Vice President

1 Prudential Grace Lines
One Whitehall St
New York, N.Y. 10004
Attn: Mr. S.S. Skouras,
President

1 Bolt Beranek & Newman, Inc
50 Moulton St
Cambridge, Mass 02138
Attn: Dr. N. Brown

1 Cornell Aeronautical Lab
Applied Mechanics Dept
P.O. Box 235
Buffalo, New York 14221

Copies		Copies	
1	Electric Boat Div Gen Dynamics Corp Groton, Conn 06340 Attn: Mr. V. Boatwright, Jr.	1	National Sci Foundation Engineering Div 1800 G Street, N.W. Washington, D.C. 20550 Attn: Director
1	Esso International 15 West 51st St New York, New York 10019 Attn: Mr. R.J. Taylor Manager, R&D Tanker Dept	1	NNSB&DDCO 4101 Washington Ave Newport News, Va 23607 Attn: Tech Lib Dept
1	General Applied Sci Labs, Inc Merrick & Steward Avnues Westbury, L.I., N.Y. 11590 Attn: Dr. F. Lane	1	Sperry Systems Management Div Sperry-Gyroscope Co Great Neck, L.I., N.Y. 11020 Attn: Mr. D. Shapiro (Mail Sta G2)
1	Gibbs & Cox, Inc 21 West Street New York, N.Y. 10006 Attn: Tech Lib	1	Society of Naval Architects & Marine Engineers 74 Trinity Place New York, N.Y. 10006
2	Grumman Aircraft Engr Corp Bethpage, L.I., N.Y. 11714 Attn: Mr. W. Carl	2	SWRI, 8500 Culebra Rd San Antonio, Texas 78206 1 Dr. H. Abramson 1 Applied Mechanics Review
4	Hydronautics, Inc Pindell School Rd Howard County Laurel, Md 20810 1 Mr. P. Eisenberg 1 Mr. M. Tulin 1 Mr. J. Dunne 1 Mr. J.O. Scherer	1	Sun Shipbuilding & DD Co Chester, Pa 18013 Attn: Mr. F. Pavlik Chief Naval Architect
1	Lockheed Missile & Space Co P.O. Box 504 Sunnyvale, Calif 94088 Attn: Mr. R. Ward Facility #1, Dept 57-01, Bldg 150	1	Stanford Research Institute Menlo Park, Calif 94025 Attn: Lib
1	Oceanics, Incorporated Technical Industrial Park Plainview, L.I., N.Y. 11803 Attn: Dr. Paul Kaplin	1	Cambridge Acoustical Associates, Inc 129 Mount Auburn St Cambridge, Mass 02138 Attn: Mr. M.C. Junger
2	McDonnell Douglas Aircraft Co Douglas Aircraft Div 3855 Lakewood Blvd Long Beach, Calif 90801 1 Mr. John Hess 1 Mr. A.M.O. Smith	1	Institute for Defense Ana 400 Army-Navy Drive Arlington, Va 22202 Attn: Mr. A.J. Tachmindji
		1	Litton Systems, Inc P.O. Box 92911 Los Angeles, Calif 90007
		1	Puget Sound Bridge & DD Co Seattle
		1	Douglas Aircraft Co., Gen Appl Sci Lab Westbury, L.I., N.Y.

Copies

1 ITEK Corp., Vidya Div.,
Palo Alto

1 George G. Sharp, Inc

1 Martin Co., Baltimore

1 Boeing Aircraft, AMS Div.,
Seattle

1 United Aircraft, Hamilton
Standard Div.,
Windsor Locks, Conn

1 AVCO, Lycoming Div.,
Washington

1 Baker Mft., Evansville

1 Tetra Tech, Inc
603 Rosewood Blvd
Pasadena, Calif 91107
Attn: Dr. Chapkis

1 Aerojet-General Corp
1100 W. Hollyvale St
Azusa, Calif 91702
Attn: Mr. J. Levy
Bldg 160, Dept 4223

1 Bethlehem Steel Corp
Central Technical Div
Sparrows Point Yard
Sparrows Point, Md 21219
Attn: Mr. A. Haff
Technical Manager

1 Bethlehem Steel Corp
25 Broadway
New York, New York 10004
Attn: H. de Luce

1 National Steel & Shipbldg Co
Habor Drive & 28th St
San Diego, Calif 92112

1 Bird-Johnson Co
883 Main Street
Walpole, Mass 02081

1 Propulsion Systems Inc
14 Vauderveutes Ave
Port Washington, N.Y. 11050

1 Baldwin-Liwa-Hamilton Corp
Industrial Equipment Div
Philla, Pa 19142

Copies

1 Propellers Incorp
77 River St
Hoboken, N.J. 07030

1 Lips, Incorp
Fifty Broad St
New York, N.Y. 10004

CENTER DISTRIBUTION

Copies	Code
1	15
1	152
1	1528
1	154
1	1544
1	156
1	1502

UNCLASSIFIED
Security Classification

DOCUMENT CONTROL DATA - R & D

(Security classification of title, body of abstract and indexing annotation must be entered when the overall report is classified)

1. ORIGINATING ACTIVITY (Corporate author) DAVID W. Taylor Naval Ship Research & Development Center Bethesda, Maryland 20034		2a. REPORT SECURITY CLASSIFICATION UNCLASSIFIED	
		2b. GROUP N/A	
3. REPORT TITLE 6 BLADE SPINDLE MOMENT ON A FIVE-BLADED CONTROLLABLE-PITCH PROPELLER.			
4. DESCRIPTIVE NOTES (Type of report and inclusive dates) 9 Research and development rept.			
5. AUTHOR(S) (First name, middle initial, last name) 10 Stephen B. Denny John J. Nelka			
6. REPORT DATE 11 Jan 72		7a. TOTAL NO. OF PAGES 32	7b. NO. OF REFS 3
8a. CONTRACT OR GRANT NO. 17 SF 35 432 D08		9a. ORIGINATOR'S REPORT NUMBER(S) 16 F35432 3729 14 SPD-3729	
b. PROJECT NO. Task 3741		9b. OTHER REPORT NO(S) (Any other numbers that may be assigned this report)	
c. Work Unit 528 009		d.	
10. DISTRIBUTION STATEMENT APPROVED FOR PUBLIC RELEASE: DISTRIBUTION UNLIMITED.			
11. SUPPLEMENTARY NOTES		12. SPONSORING MILITARY ACTIVITY Naval Ship Systems Command 03413B Washington, D.C. 23060	
13. ABSTRACT Blade spindle-moment values are presented for the operation of a five-bladed controllable-pitch propeller over a range of blade pitches and advance conditions. Spindle moment (blade turning effort) was measured on a single blade of NSRDC Model Propeller 4402 in an experimental program conducted in the 24-in. variable-pressure water tunnel. Experimental results are presented as mean spindle-moment values taken at steady-state operating conditions. No transient or time-dependent data were taken. The operating conditions investigated (1) positive pitch--steady ahead, (2) negative pitch--steady backing, and (3) negative pitch--ahead advance. The spindle moment due to hydrodynamic loading and that due to centrifugal forces were separated and nondimensionalized. The effects of Reynolds number and propeller blade cavitation are discussed briefly.			

not

14. KEY WORDS	LINK A		LINK B		LINK C	
	ROLE	WT	ROLE	WT	ROLE	WT
Spindle moment Propeller Controllable pitch Blade turning effort						